Electrochemical Studies of Copper Corrosion Inhibition in Aqueous Solution by Basic Red 46 Dye and Evaluation of the Inhibitor Adsorption Behavior

Habib Ashassi-Sorkhabi[1*], Elnaz Asghari[1] and Rana Bakhshi[1]

[1]*Electrochemistry Research Laboratory, Physical Chemistry Department, Faculty of
Chemistry, University of Tabriz, Tabriz, Iran.*

Authors' contributions

*This work was carried out in collaboration between all authors. Author HAS designed and
supervised the study and wrote the protocol. Authors EA and RB performed the statistical
analysis. Authors EA wrote the first draft of the manuscript. Author HAS wrote the final draft
of the manuscript. All authors managed the literature searches. All authors read and
approved the final manuscript.*

Original Research Article

ABSTRACT

Aims: The corrosion inhibition performance of an organic dye, Basic Red 46, was studied
against the corrosion of copper in 1M HCl. The adsorption isotherm of the used dye was
also evaluated.
Study Design: Electrochemical methods were used for this study. The corrosion of
copper sheets in HCl solution was investigated in the absence and presence of the
organic dye.
Place and Duration of Study: Electrochemistry lab., department of physical chemistry,
Chemistry Faculty, University of Tabriz, between 2009 to 2010.
Methodology: Electrochemical Impedance Spectroscopy, EIS and Tafel Polarization
techniques were used to investigate the inhibition efficiency of Basic Red 46. The copper
sheets were cut into 1×1 cm pieces, polished carefully and immersed in 1M HCl solution
for 30 minutes. Then, the EIS and polarization tests were carried out and the inhibition
efficiencies were calculated.

*Corresponding author: Email: habib.ashassi@gmail.com, ashassi@tabrizu.ac.ir;

Results: It was found that the Basic Red 46 to have good inhibiting properties for copper corrosion in acid, with efficiency between 83-88 % at a dye concentration of 400 ppm. The Langmuir adsorption isotherm could describe the dye adsorption on copper surface. Gibbs energy, ΔG_{ads}, and equilibrium constants of inhibitor adsorption on copper surface were also calculated.

Conclusion: Since ΔG_{ads} value obtained is very close to -40 kJ, it is possible to conclude that in addition to physical interactions, chemical effects may also exist. The nitrogen atoms of the molecule are suitable sites for interaction of dye with metal surface.

1. INTRODUCTION

The copper and its alloys such as brass, aluminum bronzes and Cu-Ni alloys are widely used in different industrial plants, containers, pipes, etc. Therefore, these alloys are faced to different acidic, neutral and basic corrosive conditions. One of the most important practical ways for corrosion control in the industrial environments is the addition of corrosion inhibitors to the corrosive solution. Several authors have investigated the corrosion inhibition of copper alloys in different solutions [1-5]. The corrosion inhibition of copper alloys has been studied using different organic inhibitors, mostly those containing heteroatoms such as oxygen, nitrogen and sulfur and/or aromatic compounds. The compounds such as tetrazoles [6], benzotriazoles [7,8], ketene dithioacetal derivatives [9], triazoles [10], etc are widely used as corrosion inhibitors for different copper alloys.

The aim of the present work was to investigate the inhibition performance and adsorption mechanism of an organic dye with the chemical name of N-benzyl-4-[(1,4-dimethyl-1,5-dihydro-1,2,4-triazol-1-ium-5-yl)diazenyl]-N-methylaniline bromide and commercial name of Basic Red 46, BR46, on the corrosion of copper in hydrochloric acid solution using electrochemical impedance spectroscopy and Tafel polarization techniques. BR46 like other Basic (Cationic) Dyes is water soluble and is mainly used to dye acrylic fibers as well as for direct printing. The bioremoval of this dye from wastewaters by anaerobic sludge's, duckweeds and other organisms has been studied [11-13].

2. MATERIALS AND METHODS

The pure copper bars with diameter of 1cm were cut and mounted in a polyester resin, in such a way that only a 0.785 cm^2 area disc was left uncovered. This assembly was used as working electrode in a three-electrode configuration for electrochemical measurements. A platinum rod and a saturated calomel electrode (SCE) were used as counter and reference electrodes, respectively. The corrosive solution was 1M hydrochloric acid solution made from 37% hydrochloric acid (Merck Co.). The copper discs were abraded with SiC paper up to grade 2000, deoxidized using an acidic hydrogen peroxide solution, degreased with ethanol, finally rinsed with distilled water and immersed in the corrosive solution. The inhibited solutions were prepared with different concentrations of BR46 (with the Molecular weight of 400 g/mol) including 40, 200, and 400 ppm in 1M hydrochloric acid solution. The temperature was kept at 25±1ºC using a MEMERT thermostat.

The AUTOLAB PGSTAT30 potentiostat-galvanostat was used for electrochemical measurements. Before each test, the working electrode was immersed in the test solution under open circuit conditions, until reaching to an almost steady state potential (equilibrium open circuit potential, OCP). This immersion time was found to be 30 minutes in all experiments. During this time, the OCP of working electrode was recorded versus time. Just after 30 min. immersion, the electrochemical impedance spectroscopy (EIS) tests were performed at OCP using the frequency response analyzer, FRA, module in AUTOLAB PGSTAT30. These tests were carried out in a frequency range of 100 kHz to 10 mHz in the constant potential of OCP with an ac voltage amplitude of ±10 mV. The experimental data were analyzed proposing the appropriate equivalent circuit models using Zview2 software. The Tafel polarization measurements were also made after EIS tests. The potential was swept in the range of E_{ocp} ±200 mV with a scan rate of 1mV/s.

3. RESULTS AND DISCUSSION

3.1 Tafel Polarization Measurements

Fig. 1 shows the Tafel polarization plots obtained for copper corrosion in blank and inhibited solutions. It is seen that there are current plateaus in the cathodic branch of these plots. It is well known that for copper corrosion in an aerated acidic solution, the oxygen is the main cathodic reagent and its reduction is the main cathodic reaction. The cathodic plateaus in polarization plots can be attributed to the diffusion-controlled oxygen reduction reaction. It is seen that the current on plateaus is not constant and increases slightly with potential changes; such a behavior is called a non-ideal diffusion phenomenon. The ideal diffusion theoretically causes the current density to become constant at approximately -50 mV far from OCP. For a non-ideal diffusion controlled Tafel plot, corrosion current data are estimated values that can only be used for comparison purposes not for calculation of real corrosion rates. Under these conditions, the intersection of linear extrapolations for both branches at OCP shows the estimated corrosion current [14]. Therefore, the estimated corrosion current density, i_{corr} and corrosion potential, E_{corr}, have been obtained from the curves shown in Fig. 1 and are listed in the Table 1.

Table 1. Electrochemical parameters for copper corrosion in 1 M HCl solution in the absence and presence of different concentrations of Basic Red 46 obtained from Tafel Plots

C_{inh} (ppm)	E_{corr} (mV/SCE)	i_{corr} (µA cm^{-2})	η_p%
Blank	-480	30.0	----
40	-505	16.0	47
200	-521	6.5	78
400	-523	5.0	83

It has long been known that when copper corrodes in an aerated, chloride-containing solution, a layer of copper (I) oxide, Cu_2O, is formed on the surface of the metal. In addition, copper is dissolved by reactions, which can be summarized as follow [15]:
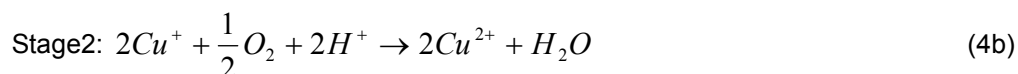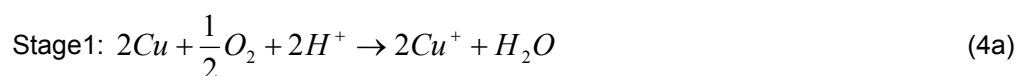
Anodic reaction: $Cu \rightarrow Cu^+ + e$ (1)

$$\text{Cathodic reaction: } \frac{1}{2}O_2 + 2H^+ + 2e \rightarrow H_2O \tag{2}$$
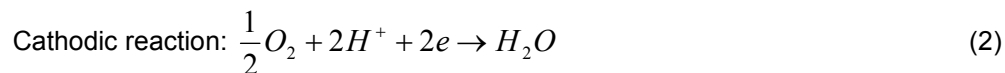
Then in the solution:

$$2Cu^+ + \frac{1}{2}O_2 + 2H^+ \rightarrow 2Cu^{2+} + H_2O \tag{3}$$

Copper ions also form complexes with chloride ions during or after reactions 1 and 3. Therefore, in acidic non-deaerated solution, the corrosion is initiated by oxygen and proceeds in two stages [15]:

$$\text{Stage1: } 2Cu + \frac{1}{2}O_2 + 2H^+ \rightarrow 2Cu^+ + H_2O \tag{4a}$$

$$\text{Stage2: } 2Cu^+ + \frac{1}{2}O_2 + 2H^+ \rightarrow 2Cu^{2+} + H_2O \tag{4b}$$

In the presence of metallic copper, the *Cu (II)* cations are subject to dismutation, which is competitive in corrosion:

$$\text{Dismutation: } Cu^{2+} + Cu \rightarrow 2Cu^+ \tag{5}$$

Insoluble copper (I) chloride, *CuCl*, precipitates on the surface of copper in the presence of chloride anions:

$$Cu^+ + Cl^- \rightarrow CuCl(s) \tag{6}$$

This insoluble layer acts as protective barrier against oxidation of copper. This copper (I) chloride, *CuCl$_{(s)}$*, layer is stable in neutral solutions but is destroyed in the acidic solutions. In the presence of high concentrations of chloride anion, the following equilibrium is also dragged in the forward direction and copper (I) chloride, *CuCl$_{(s)}$*, is destroyed [15]:

$$CuCl + Cl^- \rightarrow CuCl_2^- (surface) \rightarrow CuCl_2^- (solution) \tag{7}$$
$$\downarrow$$
$$Cu^{2+} + 2Cl^- + e$$
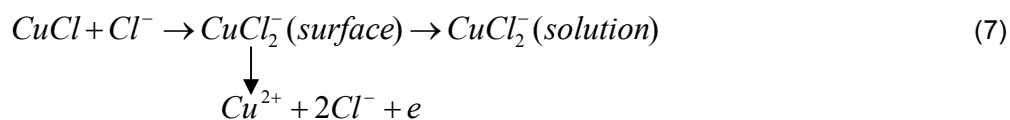
Lee and Nobe [16] found that $CuCl_3^{2-}$ and $CuCl_4^{3-}$ cuprous chloride complexes can also be produced from $CuCl_2^- (solution)$ as chloride ion concentrations become greater than 1.0 M:

$$CuCl_2^- + Cl^- \rightarrow CuCl_3^{2-} \tag{8}$$

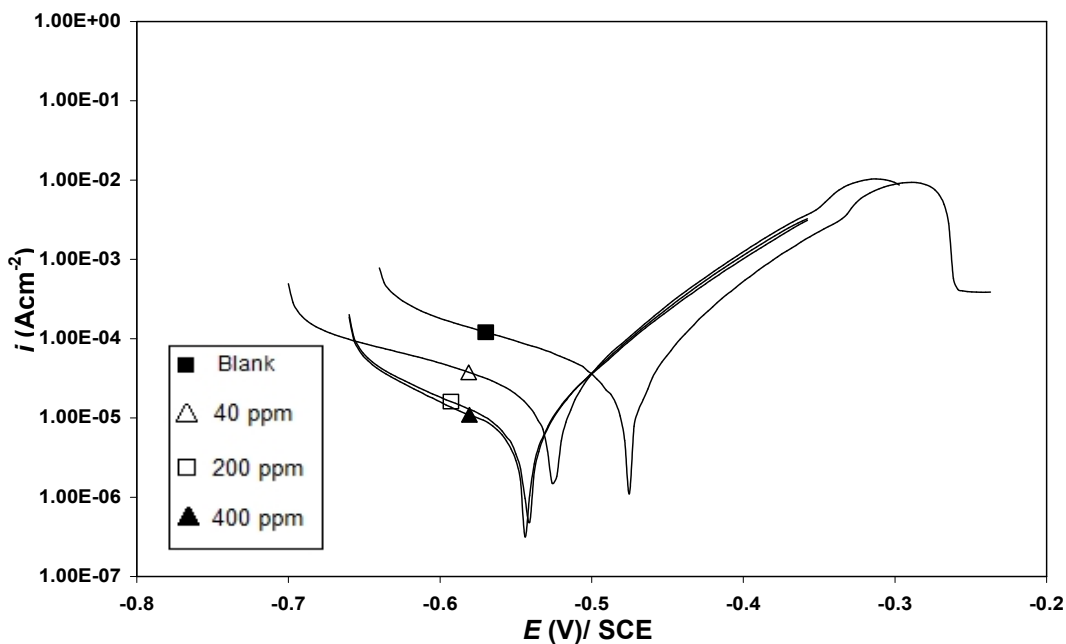$$CuCl_3^{2-} + Cl^- \rightarrow CuCl_4^{3-} \tag{9}$$

Fig. 1. Tafel polarization plots for copper corrosion in 1M HCl solution in the absence (blank) and presence of different concentrations of Basic Red 46 dye

The corrosion of copper in acidic chloride-containing solutions is also influenced by factors such as dissolved oxygen, chloride concentration and the pH of the solution. As noted in the beginning of this section, Fig. 1 shows cathodic current plateaus, which are due to the diffusion controlled reduction reaction of dissolved oxygen (equation 2) from bulk of solution toward the copper surface [17]. In a potential range of 200 mV with respect to the corrosion potential, an active anodic dissolution is obtained in the anodic branch. At potentials far from the corrosion potential, an anodic current plateau is also observed. This sudden decrease of the anodic current is due to the passivation of copper surface because of cuprous oxide and insoluble copper(I) chloride, *CuCl(ads)*, precipitation on the copper surface [10].

In the presence of BR46, the E_{corr} shifts toward the more negative values. It is also seen that, the cathodic current density decreased in the presence of BR46, while, the anodic one has not be varied significantly. This observation reveals that the BR46 acts as a cathodic organic inhibitor. The cathodic inhibitors reduce the corrosion rate through the influencing on the cathodic sites of metal surface and reducing the rate of cathodic reaction, i.e. the oxygen reduction in this case. Fig. 2 indicates a schematic Evans diagram, showing that how a cathodic inhibitor causes the reduction of i_{corr} and displacement of E_{corr} toward negative values.

The inhibition efficiencies that are listed in Table 1 were calculated from Tafel polarization data using the following equation [18]:

$$\eta_{p}\% = \left(\frac{i_{corr}^{\circ} - i_{corr}}{i_{corr}^{\circ}} \right) \times 100 \tag{10}$$

where i_{corr}° and i_{corr} are the corrosion current densities in the absence and presence of inhibitor, respectively.

It is seen that an increase in the inhibitor concentration leads to the decrease in i_{corr}. Since the organic inhibitors mostly act through adsorption on metal surface, an increase in the inhibitor concentration leads to more coverage of the metal surface, therefore the inhibition efficiency increases.
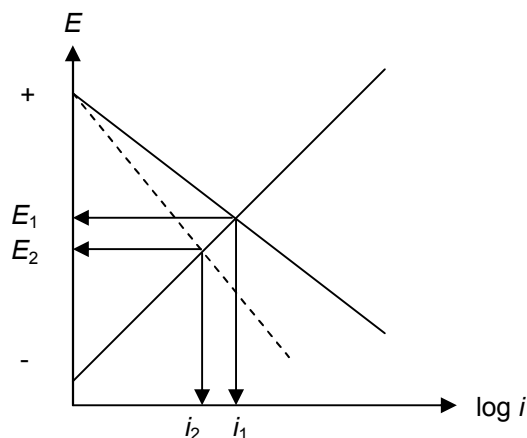

Fig. 2. The schematic Evans diagram illustrating the effect of a cathodic inhibitor on corrosion potential, E_{corr}, and corrosion current density, i_{corr}

3.2 Electrochemical Impedance Spectroscopy Measurements

The EIS measurements were also performed for copper in blank and inhibited hydrochloric acid solutions. Fig. 3 shows the obtained Nyquist diagrams for copper corrosion in blank and in the presence of different concentrations of BR46. The experimental data were analyzed using Zview2 software and proper equivalent electrochemical circuit was proposed for each case. The results for corrosion of copper in blank solution were fitted to the circuit model shown in Fig. 4a. In the Nyquist plot of copper in blank solution (Fig. 3), two capacitive loops are seen. The high frequency loop is attributed to the corrosion of copper and is fitted as a charge transfer resistance, R_{ct}, in parallel with a constant phase element, CPE_1, resulted from the double layer capacitance, C_{dl}. The R_{ct} is inversely relative to the corrosion rate of the sample. Because of the depressed shape of the capacitive loop, the constant phase element, CPE, including a component $Q_{\circ}$ and a coefficient, n, is required instead of the C_{dl} in circuit model. The CPE behavior causes by different physical phenomena like surface inhomogenities resulting from the surface roughness, impurities, porous layer formation, etc. The admittance of a CPE, Y_{CPE}, is related to $Q_{\circ}$ and n with the following relationship:

$$Y_{CPE} = Q_{\circ}(j\omega)^{n}$$

(11)

$Q_{\circ}$ and n value are frequency independent. n which takes values between 0 and 1 is a measure of surface inhomogeneity. The case $n = 1$ describes an ideal capacitor while the case $n = 0$ describes a pure resistor.
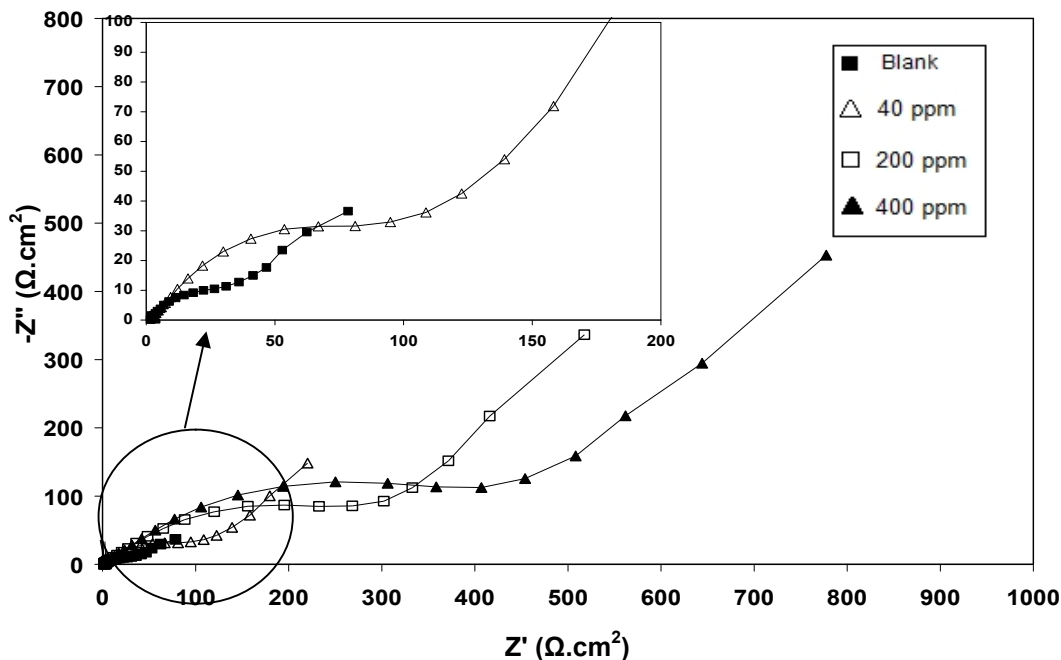
Fig. 3. The Nyquist plots for corrosion of copper in 1M HCl solution in the absence (blank) and presence of different concentrations of Basic Red 46 dye (The inset: magnified Nyquist plots for corrosion of copper in 1M HCl (Blank v) and in a 0.0001M Basic Red 46 (△) solutions)

The low frequency loop, in the Nyquist plot of copper corrosion in blank solution (Fig. 3), may be due to the adsorption of the copper (I) chloride (*CuCl*) on copper surface. This adsorption process led to a low frequency loop and is shown as a resistance, R_{ads}, in parallel with a capacitance, C_{ads} that has been shown as CPE_2 in Fig. 4a. The R_s in the equivalent circuit shows the solution resistance.

The experimental data obtained in the inhibited solution, did not show an acceptable fitting to the equivalent circuit shown in Fig. 4a. Therefore, the circuit indicated in Fig. 4b was used to fit these data. This model is consisted of a solution resistance, R_s, charge transfer resistance, R_{ct}, constant phase element of double layer, *CPE*, and a Warburg diffusion element, W. The values obtained for all circuit parameters after fitting are listed in Table 2. The R_w values in Table 2 are the resistance corresponding to the Warburg diffusion element.

It is known that the diffusion in electrochemical systems can occur in different ways. The diffusion of species such as dissolved oxygen and/or inhibitor molecules from bulk of solution toward the electrode surface and through the coprous oxide layer on metal surface leads to a 45-degree line at high frequencies in the Nyquist plot. The *n* values around 0.5 for a *CPE* also shows a diffusion behavior. It is seen from Table 2 that the *n* values for CPE_1 in all cases are around 0.5. It means that there is also finite length diffusion at low frequencies [19,20].
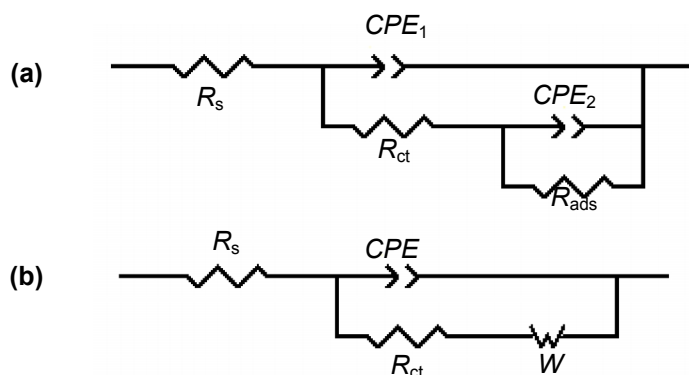
Fig. 4. Equivalent electrical circuits for describing the behavior of copper in 1M HCl solution (a) in the absence and (b) in the presence of Basic Red 46 dye

The inhibition efficiencies (η_z%) were also calculated from the R_{ct} values using the following equation [18]:

$$\eta_z(\%) = (\frac{R_{ct} - R_{ct}^0}{R_{ct}}) \times 100 \qquad (12)$$

where R_{ct}^0 and R_{ct} are the charge transfer resistances in the absence and presence of inhibitor, respectively.

It is seen from data presented in Table 2 that the R_{ct} and η_z% increase as the concentration of BR46 increases. It means that the BR46 inhibits the corrosion of copper in hydrochloric acid solution through the adsorption on the metal surface and formation of a protective layer. The R_w also enhances with the increase of inhibitor concentration because of the enhancement of the metal surface coverage and the thickness of protective layer. The trend of η_z% variation with increasing the inhibitor concentration is in agreement with the trend observed in Tafel measurements.

Table 2. Electrochemical impedance parameters for copper corrosion in 1M HCl solution in the absence and presence of Basic Red 46

C_{inh} (M)	High frequency region (loop1)			Low frequency region (loop2)				η_z%
	R_{ct} (Ω cm^2)	Q_o (Ω^{-1}cm^{-2}s^n)	n_1	R_{ads} (Ω cm^2)	$Q_{o(ads)}$ (Ω^{-1}cm^{-2}s^n)	n_2	R_w (Ωcm^{2}s$^{-0.5}$)	
Blank	41.9	1.2×10^{-2}	0.51	500	0.104	0.51	-----	-----
40	118.3	2.5×10^{-3}	0.57	-----	-----	-----	486	64
200	262.2	2.3×10^{-3}	0.52	-----	-----	-----	614	84
400	352.0	1.2×10^{-3}	0.54	-----	-----	-----	1034	88

3.3 Geometry Studies

In order to get more information on the probable centre of adsorption, the structure of the BR46 dye was optimized by applying PM3 semi-empirical method using the HyperChem Release 7.0 molecular modeling software. The optimized structure of BR46 molecule and the partial atomic charges of its heteroatoms (nitrogen atoms) are given in Fig. 5.

Fig. 5. The optimized structure of basic red 46 molecule and the partial atomic charges of its heteroatoms

In the chloride containing solution, the metal surface has negative charge because of the adsorbed chloride ions on the surface. Therefore, the nitrogen atoms that have positive partial charges are suitable sites for adsorption of the whole BR46 molecule on the metal surface.

3.4 Adsorption Isotherm

The adsorption isotherms can also provide basic information on the interaction of inhibitor molecules and metal surface [21]. The surface coverage, ($\theta = \eta\%/100$), values for each concentration of inhibitor were calculated from both polarization and EIS measurements [21,22]. Similar to the trend of inhibition efficiencies, the surface coverage of copper increases as the inhibitor concentration enhances.

The data were then tested graphically for fitting a suitable adsorption isotherm. The most common isotherms such as Langmuir and Freundlich were examined. It was found that the plots of C_{inh}/θ versus C_{inh}, from both polarization and EIS results, yields straight lines. These plots as well as the corresponding equations and regression coefficients are shown in Fig. 6.

$$y = 1.1008x + 9.62E-05$$
$$R^2 = 0.9999$$

(a)

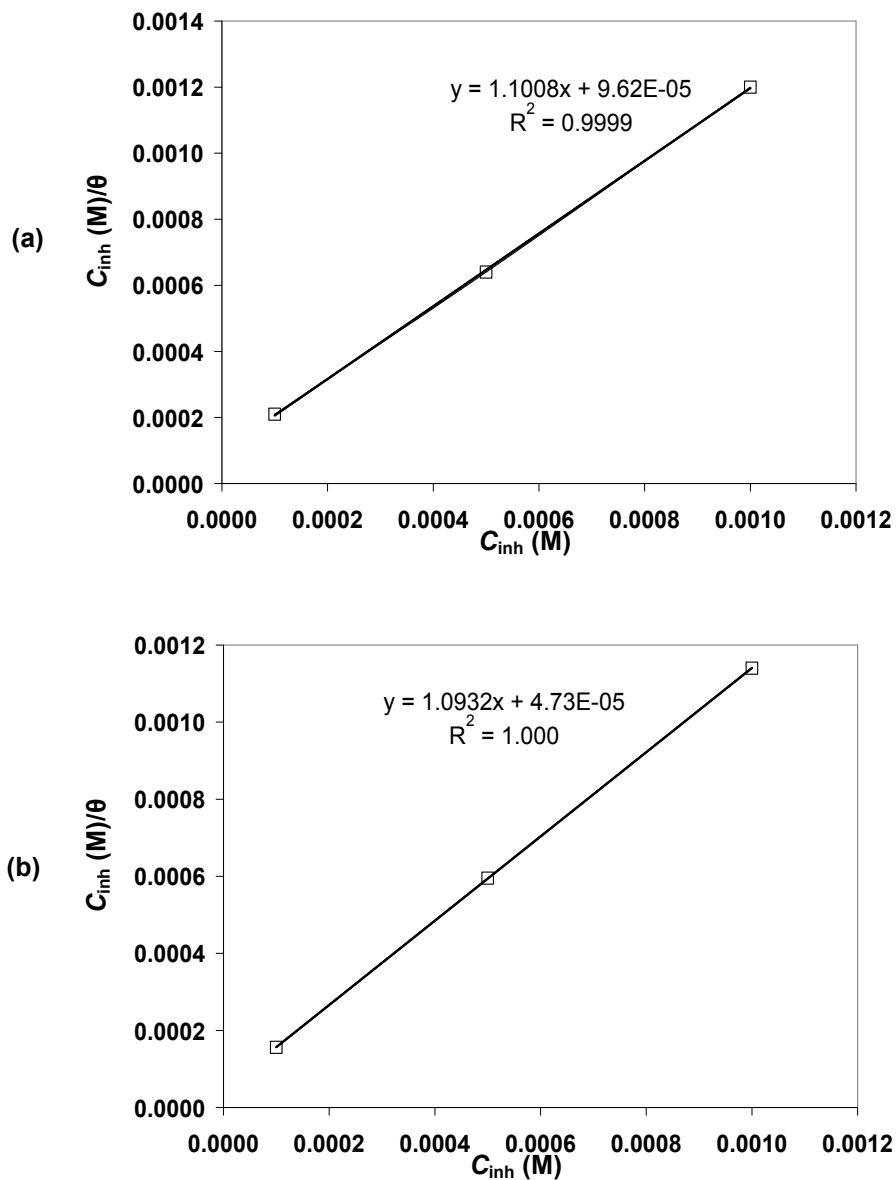

$$y = 1.0932x + 4.73E-05$$
$$R^2 = 1.000$$

(b)

Fig. 6. Langmuir isotherm plots for adsorption of basic red 46 on copper surface (a) from polarization results and (b) from EIS results

It can be deduced that adsorption of BR46 dye on the surface of copper in 1 M hydrochloric acid solution obeys the Langmuir adsorption isotherm, which is presented by the equation below [21].

Fig. 4. Equivalent electrical circuits for describing the behavior of copper in 1M HCl solution (a) in the absence and (b) in the presence of Basic Red 46 dye

$$\frac{C_{inh}}{\theta} = C_{inh} + \frac{1}{K_{ads}} \tag{13}$$

where C_{inh} is the inhibitor concentration, θ is the degree of coverage of metal surface, and K_{ads} is the equilibrium constant for adsorption–desorption process. The values of θ are proportional to the inhibition efficiencies ($\theta = \eta\%/100$). The equilibrium constants, K_{ads}, were calculated from the reciprocal of the intercept of the isotherm line. The free energy of inhibitor adsorption, ΔG_{ads}, on copper surface can be evaluated using the following equation [21]:

$$\Delta G_{ads} = -RT \ln(55.5 K_{ads}) \tag{14}$$

The values of K_{ads} and ΔG_{ads}, obtained from polarization and EIS results, as well as their average values are listed in Table 3.

Table 3. The values of K_{ads} and ΔG_{ads} for adsorption of Basic Red 46 on copper from polarization and EIS data and the average values

Polarization		EIS		Average	
K_{ads} (M^{-1})	ΔG_{ads} (kJ mol^{-1})	K_{ads} (M^{-1})	ΔG_{ads} (kJ mol^{-1})	K_{ads} (M^{-1})	ΔG_{ads} (kJ mol^{-1})
1.0395×10^4	-32.9	2.1142×10^4	-34.6	1.5768×10^4	-33.8

The negative values of ΔG_{ads} indicate spontaneous adsorption of BR46 molecules on the copper surface and strong interaction between inhibitor molecules and metal surface [22].

It is well known that the values of -ΔG_{ads} around 20 kJ mol^{-1} or lower are indicative of the electrostatic interaction between charged organic molecules and the charged metal surface (i.e. physisorption); those around 40 kJ mol^{-1} or higher involve charge sharing or transfer from the organic molecule to the metal surface to form a coordinated bond (i.e. chemisorption). The value of -ΔG_{ads} for adsorption of BR46 molecules on copper surface is less than 40 kJ mol^{-1}, indicating the physical adsorption. However, since the value of -ΔG_{ads} is close to 40 kJ mol^{-1}, it could also be concluded that in addition to the electrostatic interactions, there may be some other interactions [22]. Therefore, the adsorption mechanism of the BR46 dye molecules on copper involves two types of interaction, chemisorption and physisorption [23]. According to the geometry studies (section 3.3), the nitrogen atoms are suitable sites of the inhibitor molecule for physical interaction with the metal surface. The aromatic ring may also participate in charge sharing or transfer from the dye molecule to the metal surface.

4. CONCLUSION

The corrosion inhibition performance of the Basic Red 46 dye on the corrosion of copper in hydrochloric acid solution was studied. It was shown that the dye molecule inhibits the corrosion of copper in acidic solution through retarding the cathodic reaction i.e. oxygen reduction on metal surface. The cathodic currents decrease in the presence of inhibitor but the anodic ones are not affected. The i_{corr} decreases and E_{corr} shifts toward more negative values. The Basic Red 46 dye, therefore, is a cathodic inhibitor for copper corrosion in acidic

solution. Inhibition efficiencies enhance as the inhibitor concentration enhances. Since ΔG_{ads} value is close to -40 kJ, it is possible to conclude that in addition to physical interactions, some chemical effects may also exist. The dye molecules interact with the metal surface through physical and chemical interaction and are adsorbed on the surface obeying the Langmuir adsorption isotherm. The nitrogen atoms of the dye molecule and the aromatic rings are suitable sites for interaction with metal surface.

ACKNOWLEDGEMENTS

COMPETING INTERESTS

Authors have declared that no competing interests exist.

REFERENCES

1.   Valcarce MB, Vázquez M. Phosphate ions used as green inhibitor against copper corrosion in tap water. Corros Sci. 2010;5:1413.
2.   Sherif EM, Park SM. 2-Amino-5-ethyl-1, 3, 4-thiadiazole as a corrosion inhibitor for copper in 3.0% NaCl solutions. Corros Sci. 2006;48:40-65.
3.   Vera R, Bastidas F, Villarroel M, Oliva A, Molinari A, Ramírez D, Del Río R. Corrosion inhibition of copper in chloride media by 1,5-bis(4-dithiocarboxylate-1-dodecyl-5-hydroxy-3-methylpyrazolyl)pentane. Corros Sci. 2008;50:729.
4.   Khaled KF. Studies of the corrosion inhibition of copper in sodium chloride solutions using chemical and electrochemical measurements. Mater Chem Phys. 2011;125:427.
5.   Hamed E. Studies of the corrosion inhibition of copper in Na2SO4 solution using polarization and electrochemical impedance spectroscopy. Mater Chem Phys. 2010;121:70.
6.   Sherif EM, Erasmus RM, Comins JD. Inhibition of copper corrosion in acidic chloride pickling solutions by 5-(3-aminophenyl)-tetrazole as a corrosion inhibitor. Corros Sci. 2008;50:34-39.
7.   Finšgar M, Milošev I. Inhibition of copper corrosion by 1, 2, 3-benzotriazole: A review. Corros Sci. 2010;52:27-37.
8.   Khadom AA, Yaro AS. Mass transfer effect on corrosion inhibition process of copper–nickel alloy in hydrochloric acid by Benzotriazole. J Saudi Chem Soc, Article in Press. 2011;6:13. DOI: 10.1016/j.jscs.
9.   Fiala A, Chibani A, Darchen A, Boulkamh A, Djebbar K. Investigations of the inhibition of copper corrosion in nitric acid solutions by ketene dithioacetal derivatives. Appl Surf Sci. 2007;253:9347.
10. Sherif EM, Erasmus RM, Comins JD. Corrosion of copper in aerated acidic pickling solutions and its inhibition by 3-amino-1, 2, 4-triazole-5-thiol. J Colloid Interface Sci. 2007;306:96-104.
11. Maulin P. Shah, Patel KA, Nair SS, Darji AM. Bioremoval of Azo dye Reactive Red by Bacillus spp. J Bioremediation & Biodegradation. 2013;4:3.
12. Movafeghi A, Khataee AR, Torbati S, Zarei M, Salehi Lisar SY. Bioremoval of C.I. Basic Red 46 as an azo dye from contaminated water by Lemna minor L.: Modeling of key factor by neural network. Environ Prog. 2013;32:1082.

13. Sarioglu M, Bisgi T. Decolorization of basic red 46 (BR46; azo dye) and Methylene blue (cationic dye) dyes by anaerobic sludge: biotic and abiotic processes. Proceedings of the 11th International Conference on Environmental Science and Technology Chania, Crete, Greece; 2009.
14. Tait WS, An introduction to electrochemical corrosion testing for practicing engineers and scientists. Paris O Docs Publications, Printed in United States of America; 1994.
15. Scendo M. Corros. Sci. 2005;47:27-78.
16. Lee HP, Nobe K. Kinetics and mechanisms of Cu electrodissolution in chloride media. J Electrochem Soc. 1986;133:20-35.
17. Solmaz R, Altunbaş E, Döner A, Kardaş G. The investigation of synergistic inhibition effect of rhodanine and iodide ion on the corrosion of copper in sulphuric acid solution. Corros Sci. 2011;53:3231.
18. Şahin M, Bilgic S, Yilmaz H. The inhibition effects of some cyclic nitrogen compounds on the corrosion of the steel in NaCl mediums. Appl Surf Sci. 2002;195:1.
19. Available: http://www.consultrsr.com/resources/eis/diff-o.htm, 10 December 2011.
20. Available: http://www.consultrsr.com/resources/eis/diffusion.htm, 10 December 2011.
21. Solmaz R, Kardas G, Yazici B, Erbil M. Adsorption and corrosion inhibitive properties of 2-amino-5-mercapto-1, 3, 4-thiadiazole on mild steel in hydrochloric acid media. Colloid Surface A: Physicochem Eng Asp. 2008;312:1.
22. Keleş H, Keleş M, Dehri I, Serindağ O. Adsorption and inhibitive properties of aminobiphenyl and its Schiff Base on mild steel corrosion in 0.5 M HCl medium. Colloid Surface A: Physicochem Eng Aspects. 2008;320:138.
23. Lebrini M, Traisnel M, Lagrenee M, Mernari B, Bentiss F. Inhibitive properties, adsorption and a theoretical study of 3,5-bis(n-pyridyl)-4-amino-1,2,4-triazoles as corrosion inhibitors for mild steel in perchloric acid. Corros Sci. 2008;50:473.